

($e, 2e$) triple differential cross section of Mg in coplanar symmetric geometryY. Khajuria,^{1,*} S. Sunil Kumar,² and P. C. Deshmukh²¹*School of Applied Physics and Mathematics, SMVD University, Kakryal, J&K, India*²*Department of Physics, Indian Institute of Technology-Madras, Chennai, India*

(Received 4 May 2006; published 9 February 2007)

Spin-averaged static exchange potential and modified semiclassical exchange potential have been used in the distorted-wave Born approximation to calculate the triple differential cross section of Mg ($3s^2$) in the coplanar symmetric geometry. The calculations have been carried out at impact energies ranging from ($R=$) 1.78 to 8.84 times the first ionization potential for Mg. The effect of post-collision interactions has been included by making use of the Gamow factor introduced by Whelan *et al.* [Phys. Rev. A **50**, 4394 (1994)]. Present results have been compared with recent experiments of Murray [Phys. Rev. A **72**, 062711 (2005)] and are found to be in excellent agreement with the same except for the lowest impact energy (that is, for $R=1.78$ times above the first ionization potential).

DOI: [10.1103/PhysRevA.75.022708](https://doi.org/10.1103/PhysRevA.75.022708)

PACS number(s): 34.80.Dp

INTRODUCTION

Electron impact ionization of atoms, molecules, and ions provide a very interesting diversity of phenomena because of a wide range of kinematical situations available to the three-body final state. The ($e, 2e$) technique has been applied to a wide range of targets and kinematical arrangements since the first experimental studies of this type by Ehrhardt *et al.* [1] and Amaldi *et al.* [2]. The different geometrical conditions available in the ($e, 2e$) processes give access to the different types of information. For example, the experiments in the coplanar asymmetric geometry [where the momenta \mathbf{k}_0 , \mathbf{k}_1 , and \mathbf{k}_2 of the incident, scattered, and ejected electron, respectively, are in same plane ($\phi=0$), θ_1 (scattered electron angle) is kept small, θ_2 (ejected electron angle) is varied, and the energies of the outgoing electrons are very much different ($E_1 \gg E_2$)] provide the most complete test of formalisms of ($e, 2e$) reactions to study the collision dynamics of a single-ionization process. On other hand, the experiments in which noncoplanar symmetric geometry [\mathbf{k}_2 is out of reference plane ($\mathbf{k}_0, \mathbf{k}_1$), $\theta_1 = \theta_2 = \theta$ is fixed (usually at 45°), ϕ is varied, and the outgoing electrons are kept at the same energy] is used, provide the information about the electronic structure of the target.

Since the early days of ($e, 2e$) spectroscopy, attention has largely been confined to coplanar collisions. The testing and development of the current theories has been further challenged by including the wide range of kinematical options employed (Pochat *et al.* [3], Hawley-Jones *et al.* [4], Röder *et al.* [5], Murray [6], and Murray and Read [7–11]). Recent experiments of Murray and Cvejanovic [12] and Murray [13] in the coplanar geometry on alkaline-earth-metal and alkali-metal targets have evoked a fresh interest in this problem.

The distorted-Wave Born approximation (DWBA) is very well known and has been shown to be capable of predicting accurate ($e, 2e$) cross sections for a wide variety of atomic

targets above ~ 50 eV (Whelan *et al.* [14], Khajuria and Tripathi [15]). Allen *et al.* [16] noticed that the inclusion of post-collision interaction (PCI) and the polarization of atomic targets play an important role in determining the structure. Rioual *et al.* [17] have found that the inclusion of polarization effects and PCI leads to a better agreement for neon and argon. Whelan *et al.* [18] have found good agreement between experiment and theory with PCI and polarization potential at energies ~ 1.8 – 2.2 times the ionization threshold of hydrogen in coplanar symmetric geometry. In their work the comparison of experiment and theory has been made on an arbitrary scale and hence one cannot talk about the magnitude of the ($e, 2e$) cross section.

Recently, Chauhan *et al.* [19] have carried out DWBA calculations for calcium at low energies in the coplanar symmetric geometry in which the final-state electron-electron correlation through angle-dependent effective charges and the exchange distortion in semiclassical local approximation is introduced. They have studied the exchange distortion and post-collision effects; the exchange distortion has been introduced through the local exchange potential of Furness and McCarthy [20]. Although their results qualitatively produce most of the features of the cross section in this geometry, some discrepancies with the experiment [12,13] remain.

In the present work, DWBA with spin-average static exchange potential of Furness and McCarthy [20] and a modified semiclassical exchange potential (MSCEP) of Gianturco and Scialla [21] has been employed to study the triple differential cross section of magnesium in the coplanar symmetric geometry. The effect of post-collision interaction has also been studied through the Gamow factor [18,22]. It is observed that both the potentials give very good agreement with the experiment [13] for magnesium over the entire range of data [Figs. 2(a)–2(h)] except at 13.65 eV (the lowest) impact energy ($R=1.78$ times the first ionization threshold [Fig. 2(a)]), where some discrepancies are observed at higher scattering angles (above $\sim 95^\circ$).

Rescigno *et al.* [23] have proposed a method based on two steps: (i) exterior complex scaling (mathematical transformation of the Schrödinger equation) and (ii) calculation of quantum-mechanical flux and have calculated the triple-

*Corresponding author: SMVD University, Kakryal 182121, J&K, India; Electronic address: yugalkhajuria@yahoo.co.in

differential cross section for the electron impact ionization of hydrogen atom at low-impact energy. Their approach has successfully shown that there is an excellent agreement with the experiment at 17.6 eV incident energy on an absolute scale and have clearly highlighted the need of theoretical work with this approach for the targets with a multielectron system. The same approach has been discussed in great detail by Baertschy *et al.* [24] where they have presented more results on a triple-differential cross section of hydrogen in equal-sharing coplanar geometry at 20, 25, and 30 eV. All of their calculations are in excellent agreement with the experimental data (internormalization measurement of Röder *et al.* [25]), but for 17.6 eV, they have to scale up the experimental data by a factor of 1.15 to fit with the calculated cross section. Later on Baertschy *et al.* [26] have highlighted the limitations of the flux-extrapolation method and have reported a method of extracting an ionization cross section that proved to be more significant as compared to their earlier approach. Khajuria and Tripathi [15] have already shown that the DWBA is successful in predicting the cross section of He at 64.6 eV in the equal-energy-sharing geometry. Their results are in excellent agreement with the experiment on absolute scale and those with that of scaled-convergent close-coupling treatment of Bray *et al.* [27]. Hence it will be quite useful to extend the treatment of Baertschy *et al.* [24,26] to the multielectron systems like He, Ca, and Mg at low-impact energies.

THEORY

The triple-differential cross section is a measure of probability that an $(e, 2e)$ reaction at an incident electron of energy E_0 and momentum \mathbf{k}_0 , upon collision with the target, produces two electrons (scattered and ejected) with energies E_1 and E_2 having momentum \mathbf{k}_1 and \mathbf{k}_2 satisfying the energy relation

$$E_0 = E_1 + E_2 + I, \quad (1)$$

where I is the ionization potential of the target atom.

The triple-differential cross section for coincidence detection of the two continuum electrons emerging into the directions defined by solid angles Ω_1 and Ω_2 takes the form (in atomic units)

$$\frac{d^3\sigma}{d\Omega_1 d\Omega_2 dE_1} = (2\pi)^4 \frac{k_1 k_2}{k_0} \sum_{av} [|f|^2 + |g|^2 - \text{Re}(f^* g)]. \quad (2)$$

Here, \sum_{av} represents the sum over the final states and the average over the initial magnetic and spin degeneracies. f and g are, respectively, direct and exchange amplitudes for the ionization processes and are given by

$$f \equiv \langle \chi^{(-)}(\mathbf{k}_1, \mathbf{r}_1) \chi^{(-)}(\mathbf{k}_2, \mathbf{r}_2) | V_{12} | \chi^{(+)}(\mathbf{k}_0, \mathbf{r}_1) \psi_{nl} \rangle,$$

and

$$g \equiv \langle \chi^{(-)}(\mathbf{k}_1, \mathbf{r}_2) \chi^{(-)}(\mathbf{k}_2, \mathbf{r}_1) | V_{12} | \chi^{(+)}(\mathbf{k}_0, \mathbf{r}_1) \psi_{nl} \rangle. \quad (3)$$

In the above expressions V_{12} represents the interaction potential between the incident and target electron responsible for the ionization. χ^+ and χ^- represent the distorted waves for

incoming and outgoing electrons, respectively. ψ_{nl} represents the valence nl orbital of the target.

The orbitals ψ_{nl} have been taken from the Hartree-Fock tables of Clementi and Roetti [28] for neutral atoms. The distorted wave χ^+ for the incident electrons have been generated in the exchange potential of the neutral Mg atoms and the outgoing distorted waves χ^- for the outgoing electrons are generated in the potential of the Mg ion. In the calculations of χ^+ and χ^- , the spin-average static-exchange potential of Furness and McCarthy [20] and the local density potential of Gianturco and Scialla [21] have been used. Calculations have been carried out with (1) atom potential for the scattered electron and (2) ion potential for the scattered electron.

The effect of post-collision interaction (PCI) has been taken into account by the inclusion of parameter N_{ee} , defined as [18,22]

$$N_{ee} = \frac{\gamma}{e^{\gamma} - 1},$$

where

$$\gamma = \frac{2\pi}{|\mathbf{k}_1 - \mathbf{k}_2|}.$$

The TDCS can now be simply rewritten to incorporate PCI.

$$\frac{d^3\sigma}{d\Omega_1 d\Omega_2 dE_1} = N_{ee} (2\pi)^4 \frac{k_1 k_2}{k_0} \sum_{av} [|f|^2 + |g|^2 - \text{Re}(f^* g)]. \quad (4)$$

The principal difficulty in obtaining the TDCS is posed by the nonlocal character of the exchange potential, for which Furness and McCarthy [20] suggested a replacement by a local term. The Furness and McCarthy potential has been improved significantly by Gianturco and Scialla [21] who introduced a local density approximation to the exchange potential, known as modified semiclassical exchange potential (MSCEP), which takes much better account of exchange effects even in the description of collisions at lower energies. The MSCEP of Gianturco and Scialla [21] has been compared with the static-exchange potential of Furness and McCarthy [20] for Mg at 13.65 eV and also at 67.65 eV impact energies as shown in Fig. 1. It is clear from the figure that the additional term in MSCEP reduces the attractive character of the potential.

The amplitudes (3) are evaluated in the partial wave form. The number of partial waves required to get the convergence depends upon the incident energy and the orbital. A careful check has been made by calculating the plane-wave approximation in which the distorted waves are replaced by plane waves, then the results are compared with analytical plane-wave numbers. While this is a good test of convergence it is not “full proof” since partial-wave convergence of the plane-wave approximation can sometimes be more rapid than that of the distorted-wave case. Details about the integration of the radial matrix element are described by McCarthy [29].

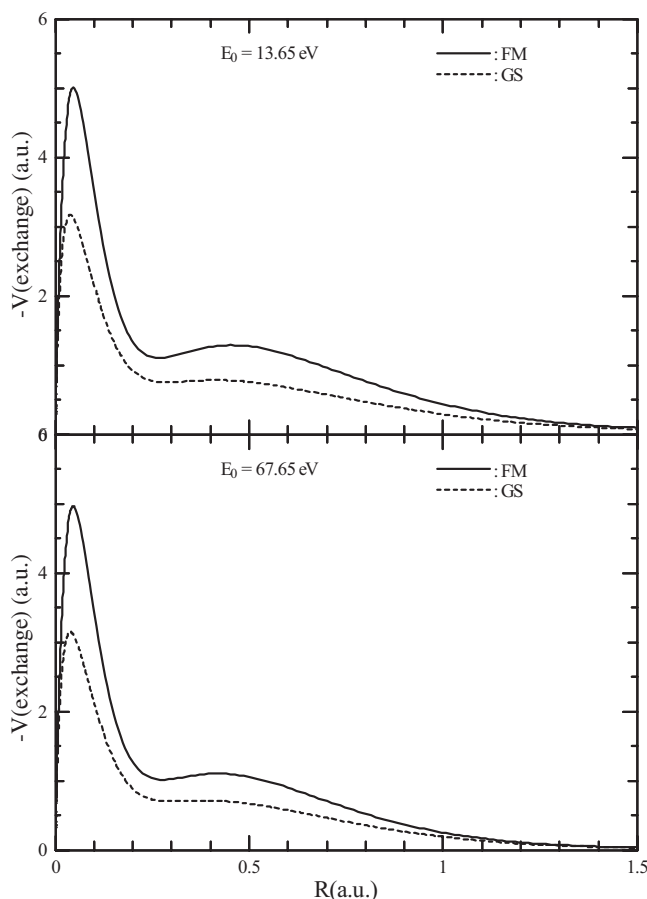


FIG. 1. Exchange part of potential at the collision energy of (a) 13.65 eV and (b) 67.65 eV. The solid line represents the static exchange potential (*FM*) [18] and the dotted line represents the modified semiclassical exchange potential (*GS*) [19].

RESULTS AND DISCUSSION

The coplanar symmetric geometry triple-differential cross section for Mg at the excess energy (E_{ex}) of 6, 10, 15, 20, 30, 40, 50, and 60 eV are presented in Figs. 2(a)–2(h) respectively, along with the recent experimental data of Murray [13]. The results are presented on a logarithmic scale because of large variations in the cross section. All the results are normalized to unity at $\theta=45^\circ$ [by simply multiplying the results (a.u.) by some numbers to make a unit cross section at $\theta=45^\circ$].

Calculations have been carried out with atom and ion potential for the fast electron with no exchange. The results with atom potential and the ion potential are almost the same; hence calculations with atom potential for the fast electron are presented here. For all the calculations, both the spin-averaged static-exchange potential and MSCEP have been used in the present study. The effect of PCI via the Gamow factor [18,22] has also been studied in the present work. The calculations using Furness and McCarthy potential enhanced by the Gamow factor [18,22] are presented in Fig. 2 and those with MSCEP potential enhanced by the Gamow factor are presented in Fig. 3.

The following features of the coplanar symmetric geometry are clearly seen from Figs. 2(a)–2(h):

(i) A forward peak at $\theta=45^\circ$ due to the single-scattering mechanism (direct collision between projectile and the target electron).

(ii) A backscattering peak at $\theta=135^\circ$ due to the double-scattering mechanism (in which the projectile first elastically scatters off the nucleus and then takes a free collision with the bound electron).

(iii) A zero cross section at $\theta=0^\circ$ and at $\theta=180^\circ$ with PCI (because of the nature of the Gamow factor).

(iv) The decrease in ratio of the forward and backward scattering peak with an increase in energy.

(v) The minimum in the cross section at $\theta=90^\circ$ (the reasons for the occurrence of this dip and other dips at a different position in this geometry might come from the strong interference between the incoming and outgoing wave function as explained earlier in the case of He [15] and Li^+ [31]).

At the excess energy of 6 eV [Fig. 2(a)] the calculated cross section shows a very good agreement with MSCEP up to $\theta=90^\circ$, where as the spin-averaged static-exchange potential shows a broader cross section in this region. At higher angles, both the potential underestimate the experimental result and the spin-averaged static-exchange potential shows a deep minimum in the cross section at $\theta=115^\circ$. The cross section that includes the PCI term is broader in the region of forward peak scattering and clearly shows the minimum cross section for $\theta=0^\circ$ and $\theta=180^\circ$. With the increase in excess energy to 10 eV [Fig. 2(b)], the agreement between the experiment and theory gets better. Both the Furness and McCarthy and Gainturco and Scialla potentials clearly predict the minimum in the cross section at $\theta=90^\circ$ in agreement with the experiment. Some discrepancies above $\theta=95^\circ$ can be seen with both potentials. Again the calculations with PCI at this energy produces a broader forward-scattering peak and minimum cross section for $\theta=0^\circ$ and $\theta=180^\circ$. For the excess energy of 15 eV [Fig. 2(c)] both the potentials produce the forward- as well as the backward-scattering peak in agreement with the experiment. The theory with both potentials predict the minimum in the cross section at $\theta=90^\circ$ and the agreement between experiment and theory at this energy is better as compared to the excess energy of 10 eV [Fig. 2(b)] for the entire set of experimental data. The calculations with PCI show the same general profile for the triple-differential cross section as it has been seen at low excess energies.

For the excess energy of 20 eV [Fig. 2(d)] the experimental cross section clearly shows the forward-scattering peak and a minimum. This minimum in the cross section is shifted by 5° as compared to the experiment at the excess energy of 10 and 15 eV. Both the potentials reproduce the cross-section shape over a relatively narrow angular range below 85° (the position of minimum in the cross section) and are in good agreement with the experiment above this angle. It is interesting to see that the cross section with PCI reproduces the experimental results in very good agreement over the complete set of experimental data. For the excess energy of 30 eV [Fig. 2(e)] both the potentials give very good agreement with the experiment over the entire set of experimental data. A relatively flat minimum in agreement with the experiment has been observed with both the potentials. The results

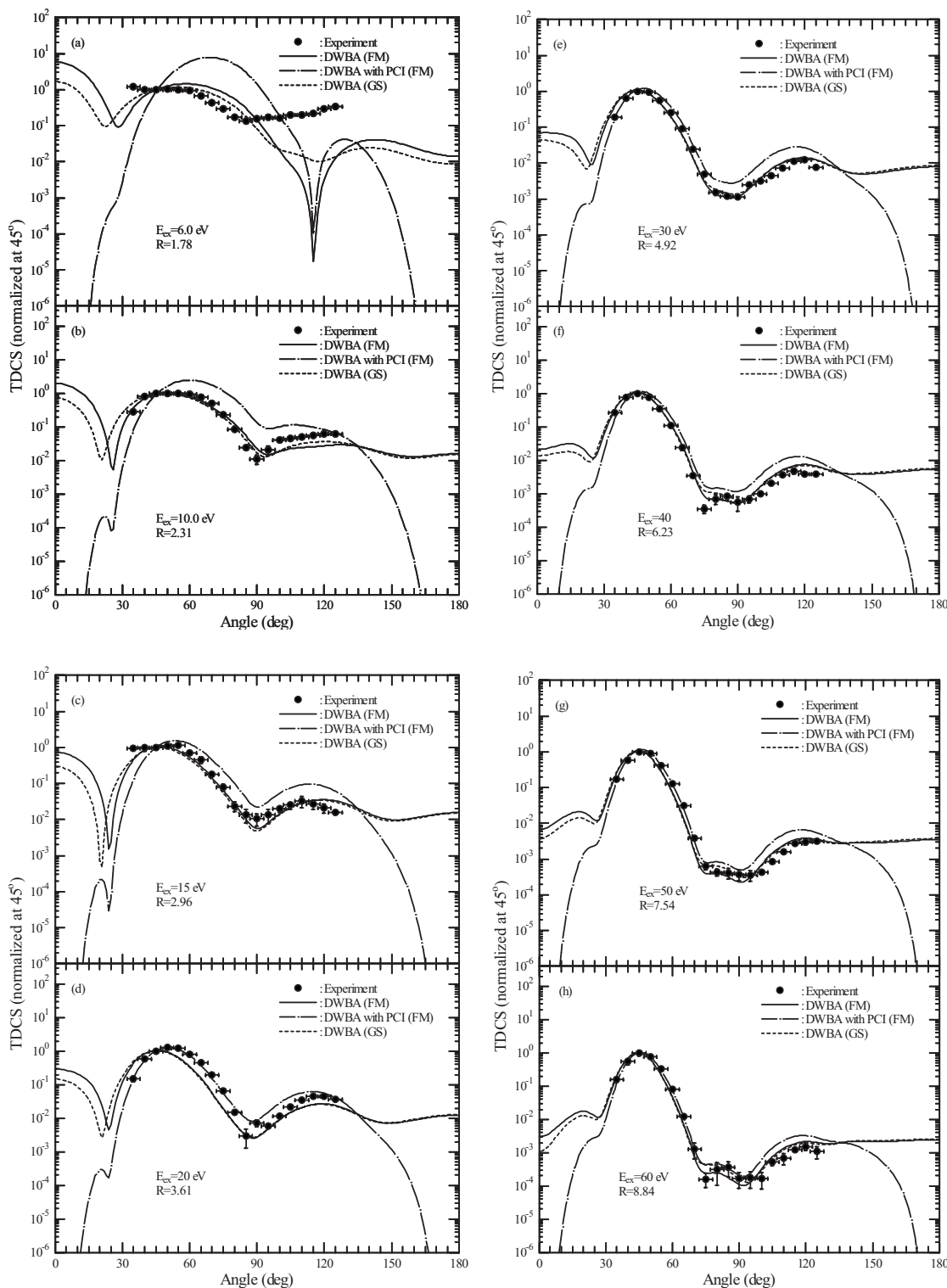


FIG. 2. Triple-differential cross section of e^- -Mg scattering at excess energies (E_{ex}) of (a) 6, (b) 10, (c) 15, (d) 20, (e) 30, (f) 40, (g) 50, (h) 60 eV. R in the figure denotes “times above the first ionization potential.” The solid line represents the calculations with Furness and McCarthy [18], the dashed line represents the calculations with modified semiclassical exchange potential [19], and the dotted line represents the calculations with PCI and spin-averaged static-exchange potential of Furness and McCarthy.

of the calculations with PCI are also in good agreement with the experiment except for the angles ($>75^\circ$) where the cross section obtained with PCI is higher than the experimental as well as the theoretical results without PCI.

The experimental cross section for the excess energy of 40 eV [Fig. 2(f)] shows a structure in the cross section between $\theta=75^\circ$ and 95° . Both the potentials show a small bump in the cross section in this region. The theoretical re-

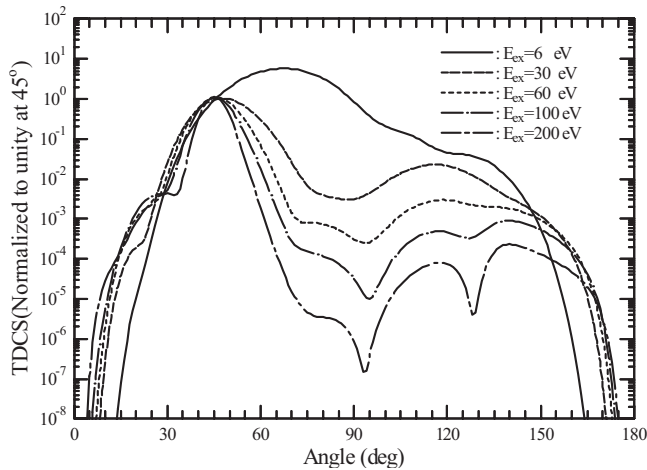


FIG. 3. Triple-differential cross section of e^- -Mg scattering with PCI and modified semiclassical exchange potential.

sults without PCI are in excellent agreement with the experiment over the entire experimental angular range, whereas the results with PCI are higher than the experiment as well as theoretical results above $\theta=75^\circ$. For the excess energy of 50 and 60 eV [Figs. 2(g) and 2(h)] the calculated cross sections without PCI are again in excellent agreement with the experiment over the entire set of experimental data. The calculations with PCI at these excess energies (50 and 60 eV) are again slightly higher than the experiment and calculations without PCI.

In the present calculations, both the potentials show a small dip in the cross section around the scattering angle of 25° . The depth of these dips increase with the decrease in the excess energy. It is also observed that the dip due to Gianturco and Scialla is shifted by 5° towards the low-scattering angle and compared to the potential due to Furness and McCarthy. Unfortunately, there is no experimental data in this region and it is therefore difficult to predict the applicability of these potentials at small angles.

To study the effect of PCI on the cross section of Mg, we plot in Fig. 3 the calculations including PCI with MSCEP at the excess energy of 6, 30, and 60 eV. In order to study this behavior in detail, calculations with excess energies of 100 and 200 eV are also presented in Fig. 3. It is clearly seen from the figure that the cross section with PCI goes to zero at $\theta=0^\circ$ and 180° . The forward-scattering peak is very broad at the lowest impact energy and lies at $\theta=68^\circ$, which becomes

narrower with an increase in excess energy to 30 eV and lies at $\theta=47^\circ$. With a further increase in energy this peaks shifts to 45° and becomes narrower. On the other hand, almost, no backward-scattering peak is observed for the lowest excess energy and a broad peak is observed for excess energies of 30 and 60 eV. For the excess energies 100 and 200 eV, the backward-scattering peak splits into two, thereby producing “three-peak” structures in the cross section. Further experimental data are needed to confirm this fact.

CONCLUSIONS

In the range of angles over which experimental data are available, both the “Furness and McCarthy” and “Gianturco and Scialla” potentials reproduce all the features of the cross section in this geometry in excellent agreement with the experiment except for the lowest excess energy (6 eV). Experimental data are required to determine the utility of both the potentials at low angles. The TDCS with electron-electron repulsion included additionally through the Gamow factor shows a vanishing cross section at $\theta=0^\circ$ and 180° . The calculated cross sections with PCI produce a broader cross section for the forward-scattering peak at low excess energies, which become narrower with the increase in the excess energy. The calculations with PCI produce a “two-peak” structure for the excess energies up to 60 eV and a three-peak structure, for the excess energies of 100 and 200 eV. The discrepancies between the experiment and the theory with PCI at low-impact energies are attributed to the nature of the Gamow factor (*Nee*). Calculations with another form of PCI introduced by Whelan *et al.* [22] in the form of the *Mee* factor and the angle-dependent form of PCI are under way. It has already been seen for He($1s^2$) [15,30] and Li $^+(1s^2)$ [31] that the minimum in the cross section for the coplanar symmetric geometry results from the interference between different scattering amplitudes. Calculations to see the same for Mg are also under way.

The present work has clearly highlighted the need for more calculations based on the procedure of Baertschy *et al.* [26] to study the triple-differential cross section for this multielectron system at low-impact energies.

ACKNOWLEDGMENT

We are thankful to Professor A. J. Murray for providing his experimental results and for useful discussions.

- [1] H. Ehrhardt, M. Schulz, T. Tekaas, and K. Willmann, Phys. Rev. Lett. **22**, 89 (1969).
- [2] U. Amaldi, Jr., A. Egidi, R. Marconero, and G. Pizzella, Rev. Sci. Instrum. **40**, 1001 (1969).
- [3] A. Pochat, R. J. Tweed, J. Peresse, C. J. Joachain, B. Piraux, and F. W. Byion, J. Phys. B **16**, 775 (1983).
- [4] T. Hawley-Jones J, F. H. Read, S. Cvejanovec, P. Hammond, and G. C. King, J. Phys. B **25**, 2393 (1992).
- [5] Roders, H. Ehrhardt, I. Bray, D. V. Farsa, and I. E. McCarthy,

J. Phys. B **29**, 2103 (1996).

- [6] A. J. Murray, in *(e, 2e) and Related Process*, edited by C. T. Whelan, H. R. J. Walters, A. Lahman-Bennan and H. Ehrhardt (Kluwer, Dordrecht, 1993), p. 372.
- [7] A. J. Murray and F. H. Read, Phys. Rev. Lett. **69**, 2912 (1992).
- [8] A. J. Murray and F. H. Read, J. Phys. B **26**, 369 (1993).
- [9] A. J. Murray and F. H. Read, Phys. Rev. A **47**, 3724 (1993).
- [10] A. J. Murray and F. H. Read, J. Phys. B **33**, 2859 (2000).
- [11] A. J. Murray and F. H. Read, J. Phys. B **33**, L297 (2000).

- [12] A. J. Murray and D. Cvejanovic, *J. Phys. B* **36**, 4875 (2003).
- [13] A. J. Murray, *Phys. Rev. A* **72**, 062711 (2005).
- [14] C. T. Whelan, H. R. J. Walters, R. J. Allan, and X. Zhang, in *(e,2e) and Related Process*, edited by C. T. Whelan, H. R. J. Walters, A. Lahman-Bennan, and H. Ehrhardt (Kluwer, Dordrecht, 1993), p. 1.
- [15] Y. Khajuria and D. N. Tripathi, *J. Phys. B* **31**, 2359 (1998).
- [16] R. J. Allan, C. T. Whelan, and H. R. J. Walters, *J. Phys. IV* **3**, 39 (1993).
- [17] S. Rioual, A. Pochat, F. Gélébart, R. J. Allan, C. T. Whelan, and H. R. J. Walters, *J. Phys. B* **28**, 5317 (1995).
- [18] C. T. Whelan, R. J. Allan, J. Rasch, H. R. J. Walters, X. Zhang, J. Röder, K. Jung, and H. Ehrhardt, *Phys. Rev. A* **50**, 4394 (1994).
- [19] R. K. Chauhan, M. K. Srivastava, and R. Srivastava, *Phys. Rev. A* **71**, 032708 (2005).
- [20] J. B. Furness and I. E. McCarthy, *J. Phys. B* **6**, 2280 (1973).
- [21] F. A. Gianturco and S. Scialla, *J. Phys. B* **20**, 3171 (1987).
- [22] C. T. Whelan, R. J. Allen, and H. R. J. Walters, *J. Phys. IV* **3**, C6–39 (1993).
- [23] T. N. Rescigno, M. Baertschy, W. A. Isaacs, and C. W. McCurdy, *Science* **286**, 2474 (1999).
- [24] M. Baertschy, T. N. Rescigno, W. A. Isaacs, X. Li, and C. W. McCurdy, *Phys. Rev. A* **63**, 022712 (2001).
- [25] J. Röder, J. Rasch, K. Jung, C. T. Whelan, H. Ehrhardt, R. J. Allan, and H. R. J. Walters, *Phys. Rev. A* **53**, 225 (1996).
- [26] M. Baertschy, T. N. Rescigno, and C. W. McCurdy, *Phys. Rev. A* **64**, 022709 (2001).
- [27] I. Bray, V. D. Fursa, J. Röder, and H. Ehrhardt, *J. Phys. B* **30**, L101 (1997).
- [28] E. Clementi and C. Roetti, *At. Data Nucl. Data Tables* **14**, 177 (1974).
- [29] I. E. McCarthy, *Aust. J. Phys.* **48**, 1 (1995).
- [30] J. Berakdar and J. S. Briggs, *J. Phys. B* **27**, 4271 (1994).
- [31] Y. Khajuria, L. Q. Chen, X. J. Chen, and K. Z. Xu, *J. Phys. B* **35**, 93 (2002).